

Simulation of an electron beam and plasma interaction*

A.A. Efimova

Abstract. The problem of an electron beam and plasma interaction, arising from the GOL-3 (BINP SB RAS) experiments, is considered. For the given problem, it is appropriate to use the collisionless plasma approach, described by a set of the Vlasov–Maxwell equations. The Vlasov equation is calculated via the particle-in-cell method. To find the electric and the magnetic fields, the Langdon–Lasinski scheme, in which fields are determined from difference approximations from the Faraday and the Ampere laws, was used. The tests made have shown that the proposed model adequately describes the plasma temperature effects.

1. Introduction

The given problem deals with investigation of the plasma thermal conductivity, where plasma is heated by a relativistic electron beam. The beam and plasma parameters were chosen close to those of the GOL-3 II experiment [1, 2]. The GOL-3 facility represents a plasma high-density thermonuclear trap of the open type in which the plasma is heated by means of a powerful relativistic electron beam. According to its parameters, plasma of the GOL-3 facility is sub-thermonuclear.

It is shown that the cooling of plasma in this facility after the heating process terminates is satisfactorily described by the classical electron heat conductivity [1]. In order to explain both the absolute value obtained in the electron temperature experiment and, the heating dynamics and the temperature distribution along the facility, suppression of the heat conductivity is required during the heating process. The suppression differs 100–1000 times in comparison with the one by classical calculations, i.e., there is a so-called abnormal heat conductivity. The presence of a high-collision frequency permits one to interpret a number of experimental data such as a fast drop (almost to zero) of the power of the mild plasma roentgen radiation [2]. There is a necessity to investigate the nature of an abnormal collision frequency for a successful planning of experiments and interpretation of acquired data.

The most probable reason of a change in plasma kinetic properties in the process of the beam injection is an electron spreading over density fluctuations, appearing during the nonlinear stage of the beam instability evolution.

*Supported by the Russian Foundation for Basic Research under Grants 08-01-00615 and 08-01-00622, and SB RAS Integration Project 113.

There are many papers concerned with investigation of the nonlinear stage of the collective relativistic electron beam and plasma interaction, but rigorous analytical results in this area have been obtained only for more or less simple physical models [3, 4]. This results in the use of the numerical modeling for solving the given problem. For this purpose, a number of codes have been developed. With these codes one solves a set of Vlasov–Maxwell equations by the particle-in-cell (PIC) method [5–7] and investigates the relaxation process of an electron beam in plasma in collisionless plasma approximation. A feature of the particle-in-cell method is a special manner of discretization, in which the number of model particles is introduced as a grid of mobile nodes [6]. Modifications of this method differ from each other by the kernel of particles, whose types are proposed in [6, 7]. In this paper, the PIC kernel is used. It is more frequently used for solving real physical problems as the numerical algorithm is simple in realization and allows one to find a sufficiently accurate solution.

The novelty of this paper consists in the temperature modeling via the PIC-method. The difficulty of the problem is that separate model particles combine a number of real particles, and, consequently, there is a problem of dispersion interpretation of a particle distribution function by velocities as temperature.

In the first section, a general problem statement is introduced. The numerical methods by which the given problem was solved are considered in the second section. Also, there are difference approximations of the corresponding equations. The methods to find the particle temperature in plasma and formulas for definition of energy are described in the third section. In the last section, the test numerical experiments are presented.

2. Problem statement

The model uses the collisionless approximation of plasma [5–7]. Plasma is described by a system of the Vlasov–Maxwell equations

$$\frac{\partial f_k}{\partial t} + (\vec{v}, \vec{\nabla}) f_k + q_k \left(\vec{E} + \frac{1}{c} [\vec{v} \times \vec{H}] \right) \frac{\partial f_k}{\partial \vec{p}} = 0, \quad (1)$$

$$\text{rot } \vec{H} = \frac{4\pi}{c} \vec{j} + \frac{1}{c} \frac{\partial \vec{E}}{\partial t}, \quad \text{div } \vec{H} = 0, \quad (2)$$

$$\text{rot } \vec{E} = -\frac{1}{c} \frac{\partial \vec{H}}{\partial t}, \quad \text{div } \vec{E} = 4\pi\rho, \quad (3)$$

$$\vec{j} = \sum_k q_k \int \vec{v} f_k(\vec{p}, \vec{r}, t) d\vec{p}, \quad \rho = \sum_k q_k \int f_k(\vec{p}, \vec{r}, t) d\vec{p}, \quad (4)$$

where f_k is a particle distribution function of the species k (electrons or ions), \vec{H} is a magnetic field, \vec{E} is an electric field, c is the speed of light,

ρ is the electric charge density, \vec{j} is the electric current density, and q_k is the charge of a particle of the species k .

Equation (1) is a collisionless kinetic Vlasov equation, equations (2), (3) are a system of the Maxwell equations, equations (4) define the current and the charge densities by particle distribution functions. It is assumed that all magnitudes depend on the spatial cartesian coordinates (x, y, z) , i.e., a three-dimensional non-stationary problem is solved. The calculation box has a parallelepiped form ($0 \leq x \leq l_x$, $0 \leq y \leq l_y$, $0 \leq z \leq l_z$) and the injection direction of a beam is along x -axis. The boundary conditions are periodic, i.e.,

$$F|_{x=0} = F|_{x=l_x}, \quad F|_{y=0} = F|_{y=l_y}, \quad F|_{z=0} = F|_{z=l_z}, \quad (5)$$

where F is any one of the following quantities \vec{E} , \vec{H} , f_k , \vec{j} , and ρ . Homogeneity conditions of the initial electron (n_e), the ion (n_i) and the beam electron densities are imposed. The distribution by ion velocities is Maxwellian, the distribution by electron velocities is a shifted Maxwellian for compensation of the beam current

$$\vec{j}|_{t=0} = 0, \quad (6)$$

where \vec{j} is defined from equation (4). At the initial time, plasma is isothermal. A system of equations (1)–(4) is a consistent integro-differential system of equations.

The PIC-method [5–7] is the most appropriate one for solving such system of equations. By using this method, plasma is simulated by a set of discrete particles, whose motion trajectories are characteristics of equation (1). Thus, the Maxwell equations and the relativistic motion equations for macroparticles need to be solved. In the dimensionless form, this system is described as follows:

$$\frac{d\vec{p}_k}{dt} = q_k(\vec{E} + \beta_0[\vec{v}_k, \vec{H}]), \quad \frac{d\vec{r}_k}{dt} = \vec{v}_k, \quad (7)$$

$$\vec{p}_k = \gamma_k m_k \vec{v}_k, \quad \gamma_k = \sqrt{1 + (p_k \beta_0 / m_k)^2}, \quad (8)$$

$$\frac{\partial \vec{H}}{\partial t} = -\frac{1}{\beta_0} \text{rot } \vec{E}, \quad \frac{\partial \vec{E}}{\partial t} = -\frac{1}{\beta_0} \text{rot } \vec{H} - \vec{j}, \quad (9)$$

$$\vec{j} = \sum_{k,i} q_k n_k \vec{v}_{i,k}, \quad (10)$$

where γ_k , m_k , and n_k are the relativistic factor, mass, and density of species k , $\beta_0 = \frac{v_0}{c}$. By finding the current in equation (10), summation is carried out by all particles and all components, $q_k n_k$ is the charge density of a macroparticle of the kind k .

The current density is found in such a manner that the continuity equation is applied at all grid points. The following relations

$$\operatorname{div} \vec{E} = 4\pi\rho, \quad \operatorname{div} \vec{H} = 0 \quad (11)$$

are automatically satisfied.

3. Numerical algorithms

3.1. Approximation of the Vlasov equation. For solving the Vlasov equation, the PIC-method [5–8] is used. In this method, plasma is modeled by a set of separate particles, each one characterizing the motion of many physical particles. Characteristics of the Vlasov equation describe trajectories of the particle motion with equations (7). To solve these equations, the following leap-frog scheme is used

$$\begin{aligned} \frac{p_k^{m+1/2} - p_k^{m-1/2}}{\tau} &= q_k \left(E^m + \beta_0 \left[\frac{v_k^{m+1/2} - v_k^{m-1/2}}{2}, H^m \right] \right), \\ \frac{r_k^{m+1/2} - r_k^{m-1/2}}{\tau} &= v_k^{m+1/2}. \end{aligned} \quad (12)$$

The PIC-method reduces the six-dimensional problem of solving the Vlasov equation to that of integration of separate particle motion equations. With finite difference methods, the time complexity of the problem solution is reduced from $O(n^6)$ to $O(n^3)$ in the PIC-method.

3.2. Approximation of the Maxwell equations. The Maxwell equations are solved using the Euler variables [7, 8]. The charge and the current densities, equations (4), which are necessary for their solution, are defined by particle velocities and coordinates

$$\rho(r, t) = \sum_{k=1}^K q_k R(r, r_k(t)), \quad j(r, t) = \sum_{k=1}^K q_k v_k(t) R(r, r_k(t)) \quad (13)$$

or in the grid form:

$$\vec{j}_i^{m+1/2} = \sum_p q_p v_p^{m+1/2} \vec{R}(x_i - x_p^{m+1/2}). \quad (14)$$

Here q_k is a charge of the particle with number k and the function $R(r, r_k(t))$ is the kernel of the PIC-method. This characterizes the particle form and size and the charge distribution [6, 7]. The PIC-kernel has been used. The current density is found in such a manner that the continuity equation

$$\frac{\partial \rho}{\partial t} + \operatorname{div}_h \vec{j} = 0 \quad (15)$$

is applied at all mesh points [7, 8]. Then the following relations are automatically satisfied

$$\operatorname{div}_h B^{m+1/2} = 0, \quad \operatorname{div}_h E^m = 4\pi\rho. \quad (16)$$

For finding the electric and the magnetic fields, the scheme offered by Langdon and Lasinski [8, 9] was used. Here fields are defined from the difference analogues to the Faraday and the Ampere laws (9):

$$\begin{aligned} \frac{H^{m+1/2} - H^{m-1/2}}{\tau} &= -\frac{1}{\beta_0} \operatorname{rot}_h E^m, \\ \frac{E^{m+1} - E^m}{\tau} &= -\frac{1}{\beta_0} \operatorname{rot}_h H^{m+1/2} - j^{m+1/2}. \end{aligned} \quad (17)$$

In this scheme, magnitudes of the electric and the magnetic fields are calculated at the mesh points, displaced regarding each other by time and space (Figure 1), $BX_{i-1/2,l,k}$, $BY_{i,l-1/2,k}$, $BZ_{i,l,k-1/2}$, $EX_{i,l-1/2,k-1/2}$, $EY_{i-1/2,l,k-1/2}$, $EZ_{i-1/2,l-1/2,k}$, where B is calculated on the shifted time step and E is calculated on the entire time step.

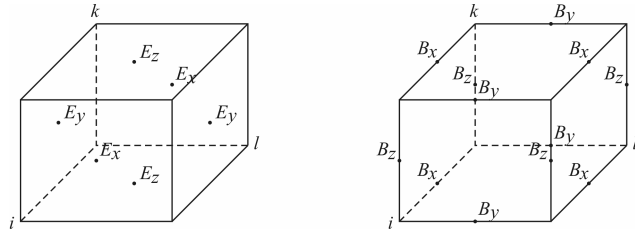


Figure 1. The scheme of displacement of the electric and the magnetic fields intensity component

The following stability condition for the scheme has been experimentally found:

$$\frac{(\beta_0 v + 1)\tau}{\beta_0 h} < 1, \quad \beta_0 = \frac{v_0}{c}. \quad (18)$$

4. Calculation technique

4.1. The calculation of energy. For the code testing, the energy conservation law was examined. The condition of the total energy conservation is found from the following equation (c.f. [10])

$$\frac{\partial}{\partial t} \left(\frac{E^2 + B^2}{8\pi} + m_i n_i c^2 \gamma_i + m_e n_e c^2 \gamma_e + m_b n_b c^2 \gamma_b \right) + \\ \text{div}(\vec{S} + m_i n_i c^2 \gamma_i \vec{v}_i + m_e n_e c^2 \gamma_e \vec{v}_e + m_b n_b c^2 \gamma_b \vec{v}_b) = 0, \quad (19)$$

where $\vec{S} = \frac{c}{4\pi} [\vec{E}, \vec{B}]$. The total energy conservation law follows from the equality to zero of the first term in equation (19):

$$W = \int \frac{E^2 + B^2}{8\pi} dV + \sum_k \int m_k n_k c^2 \gamma_k dV = \text{const}, \quad \gamma_k = \sqrt{1 + \beta_0^2 p_k^2}.$$

In the dimensionless form, the total energy can be expressed as follows:

$$W'_2 = \beta_0^2 \int \frac{E'^2 + B'^2}{2} dV' + \frac{1}{\alpha} \int n'_i \gamma_i dV' + \int n'_e \gamma_e dV' + \int n'_b \gamma_b dV'.$$

The integral for each particle species can be presented as sum of all particles. Then the equation for the total energy can be rewritten in the form

$$W = \frac{\beta_0^2}{2} h_x h_y h_z \sum_{i,l,k} (E'^2 + B'^2)_{i,l,k} + \frac{A_{m_i}}{\alpha} h_x h_y h_z \sum_{j \in i} \sqrt{1 + \beta_0^2 p_j^2} + \\ |A_{m_e}| h_x h_y h_z \sum_{j \in e} \sqrt{1 + \beta_0^2 p_j^2} + |A_{m_b}| h_x h_y h_z \sum_{j \in b} \sqrt{1 + \beta_0^2 p_j^2}, \quad (20)$$

where A_m is a dimensionless characteristic of the particle mass.

4.2. The calculation of the particle temperature. The molecule distribution law by the Maxwellian velocities describes a stationary molecule distribution of a homogeneous monoatomic ideal gas by velocities in the conditions of thermodynamic balance and the absence of the external force field. The Maxwellian molecule distribution by velocities is established as a result of mutual collisions between molecules in their chaotic thermal motion [11].

As shown in [11], the following forms of the Maxwellian distribution law are used. The molecule distribution by absolute magnitudes of velocities is

$$dn_u = n \left(\frac{m}{2\pi\kappa T} \right)^{3/2} e^{-\frac{mu^2}{2kT}} 4\pi u^2 du, \quad (21)$$

where u is the absolute value of the molecule velocity, $u = \sqrt{u_x^2 + u_y^2 + u_z^2}$, m is the molecule mass, κ is the Boltzmann constant, T is the absolute temperature, dn_u is the number of molecules (from their total number n), whose speeds are concluded within the limits from u to $u + du$. The Maxwellian distribution in the form of

$$dn = n \left(\frac{m}{2\pi\kappa T} \right)^{3/2} e^{-\frac{mu^2}{2kT}} du_x du_y du_z,$$

where u_x, u_y, u_z are coordinate components of the molecule velocity, can be rewritten as

$$dn = n f(u_x) f(u_y) f(u_z) du_x du_y du_z, \quad (22)$$

$$f(v) = \left(\frac{m}{2\pi\kappa T} \right)^{1/2} e^{-\frac{mv^2}{2kT}}. \quad (23)$$

Function (23) is a distribution function by velocity components. As all directions of the molecule motion in space are equiprobable, the molecule distribution by velocities is isotropic and has the same form for u_x, u_y , and u_z . From the formula of the distribution function (23), it can be seen that the dispersion is equal to $\frac{\kappa T}{m}$. Thus, the temperature is calculated as velocity dispersion.

5. Numerical experiments

The main task of the modeling was reproducing the heat conductivity effects of plasma. As a test, a simplified problem statement was used. Plasma consists of two species of immobile particles. In this case, the ion and the electron temperatures should be determined to the same value. A change in energy was used for the solution control, and the rates of particle velocity change were the test result.

5.1. The speed dependence of ion and electron temperature establishment from the relation of ion and electron masses. As discussed above, the ion and the electron temperature should be gradually established to the same value in the beam free plasma. The behavior of energy at the

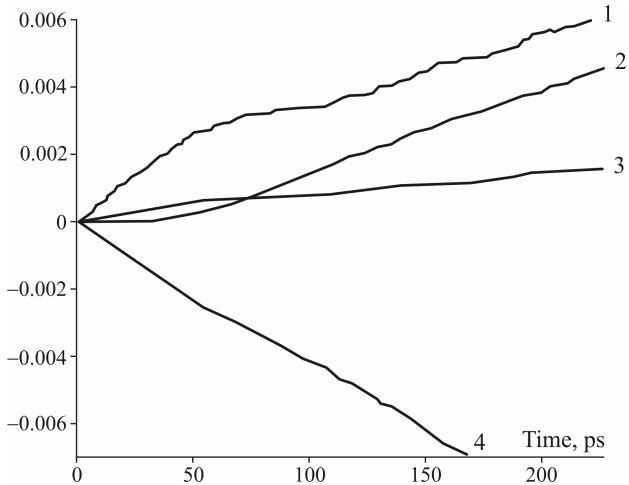


Figure 2. A change in the electric field energy (line 1), the total energy (line 2), the ion energy (line 3), and the background electron energy (line 4)

initial stage of the temperature establishment process is shown in Figure 2. The test parameters are $\alpha = m_e/m_i = 0.1$, $m_e = 9.11 \times 10^{-28}$ g is the electron mass and $m_i = 9.11 \times 10^{-27}$ g is the ion mass.

From this figure, it can be seen that the total energy conserves (an error less than 1 %), the ion energy increases and the background electron energy decreases. The magnetic field energy was neglected as it is almost zero.

In Figure 3, there are plots of dependence of the ion and the electron temperatures on time with different ion mass values. From this figure one can see that the ion and the electron temperatures are gradually established to the same value. In Figure 3a, the plot of the temperature establishment with above indicated parameters is presented. In Figure 3b the following parameters are chosen: $\alpha = 0.01$, $m_e = 9.11 \times 10^{-28}$ g, and $m_i = 9.11 \times 10^{-26}$ g. Figure 3c shows a plot of the temperature establishment using $\alpha = 1.84 \times 10^{-5}$, $m_e = 9.11 \times 10^{-28}$ g, and $m_i = 1.67 \times 10^{-24}$ g.

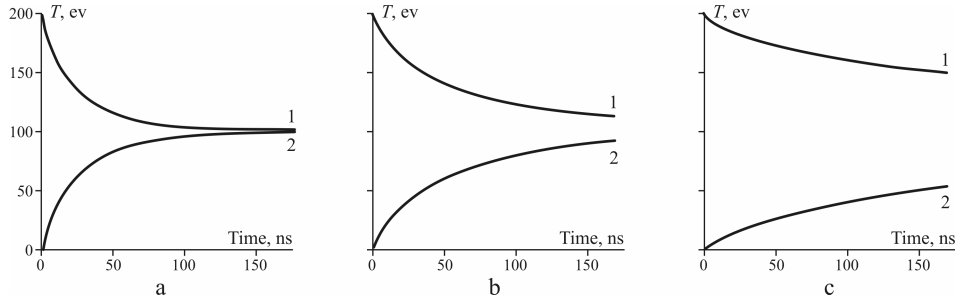


Figure 3. Establishment of the electron (line 1) and the ion (line 2) temperatures

As a result of the tests, it can be noted that the greater the relation of the electron mass to the ion mass, the slower their temperature is established. This happens because for heating the heavier ions more energy is required. The heating of ions occurs because of the fact that electrons give them a part of their energy via the electric field. Since electrons are cooled at the rate of heating ions then the rates of the ion and electron temperature establishment are the same.

5.2. Investigation of the rate of the ion and the electron temperature establishment depending on the total number of particles. The dependence of the rate of the ion and the electron temperature establishment in plasma on the total number of particles has been investigated. The key parameters for the calculation with the total number of particles of 30,000 (Figures 4 and 5) are the following: the ion density is 10^{12} cm $^{-3}$, the electron temperature is 200 eV, a characteristic length (the Debye length) is 0.033 cm, the characteristic time is 0.18×10^{-10} s, the thermal speed is 0.19×10^{10} cm/s, the density of model particles is 0.55×10^9 cm $^{-3}$, the ratio of the particles number in real plasma to that of the simulated one is 1222,

the number of model particles in the Debye cube is 30,000, $\alpha = 0.1$ (and then in calculations). The initial energy magnitudes are as follows: the ion energy is 0, the background electron energy is 2.28×10^{-10} erg, the electric field energy 5.63×10^{-19} erg, the total energy 2.28×10^{-10} erg.

The plots presented in Figure 4 show the validation of conservation laws. In this figure, the line 3 designates a change in electric field energy, the line 2 represents a change in the total energy, the line 1 indicates to a change in the ion energy, and the line 4 shows a change in the background electron energy. The total energy almost does not change.

In the course of the temperature establishment process to the one value (see Figure 5), the background electron and the ion energies go to a certain level (see Figure 4).

Also, the ion and the background electron temperatures were found for the total particle numbers equal to 40,000, 50,000, and 60,000 (Figure 6). In this figure, plots of a change in the background electron temperature are presented (the ion temperature changes with the same speed). It follows from this figure, that the rates of the temperature establishment decrease with increasing of the total number of particles.

The temperature dependence on time is exponential. The greater the total number of particles, the slower the temperature establishment, and

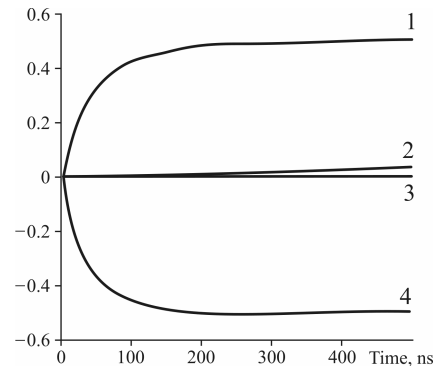


Figure 4. The change of energy

</div

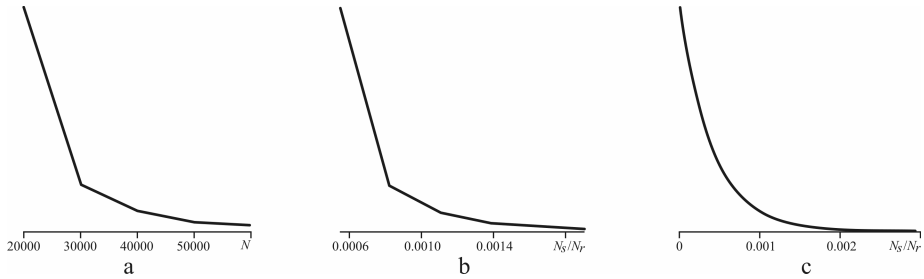


Figure 7. Plots of the exponent dependence describing the rate of temperature establishment: a) of the total number of particles; b) of the ratio of particle numbers in the real and simulated plasma; c) exponential approximation using Maple

the exponent coefficients becomes smaller. The exponent coefficients were found for all the tests. A plot of the exponent coefficient of the total particle number is shown in Figure 7a. The most demonstrative dependence is the one with the exponent coefficient of the ratio of the model particle number to the real plasma particle number. This dependence is reflected in Figure 7b. One can see that the exponent coefficient dependence, which reflects the rate of electron temperature establishment of the ratio of particle numbers in the modeling and real plasma, is also exponential (Figure 7c).

The following table represents the ratios of the total number of particles in the real plasma (N_r) and in the simulated plasma (N_s) in dependence with the total number of modeled particles (N).

N	N_r/N_s	N_s/N_r	N	N_r/N_s	N_s/N_r
20000	1834	0.00055	50000	733	0.00136
30000	1222	0.00082	60000	611	0.00164
40000	916	0.00109	70000	523	0.00191

From the presented plots, one can note that in the case when the number of simulated particles is close to that of real particles in the Debye cube, the exponent coefficient has a small value and the temperature establishment occurs very slowly.

6. Conclusion

In this paper, the model allowing one to investigate a change in the electron collision frequency during the relaxation of a relativistic electron beam in plasma is presented. The model describes only the electron heat conductivity behavior of plasma as a result of a few reasons. Because of the choice of periodic boundary conditions a continuous spectrum of the Langmuir plasma fluctuations is replaced for a discrete one. Therefore, the space area, in which waves can scatter as a result of some nonlinear process (for exam-

ple, the induced scattering on ions [3]), strongly decreases. As a result, the instability is saturated at a greater energy level (this case is entirely similar to the greater energy-conversion efficiency of the beam in magnetized plasma, in which the area of allowable scattering decreased by introducing a magnetic field [3]). This can lead to a stronger suppression of the heat conductivity coefficient in comparison with a real magnetized plasma. Large thermal fluctuations and a small number of macroparticles in the Debye sphere, which are typical of the PIC-method [5–7], restrict the region in the impulse space, in which the collision frequency is properly described. At the same time, the model is not associated, for example, with applicability conditions of the quasilinear theory. This allows one to use it for constructing various dependencies, for example, a curved qualitative dependence of a suppression degree of the beam and the plasma parameters. At the current stage of the work, the algorithm and the code were developed. They allow modeling the heat conductivity effects in plasma, including the electron and the ion temperature establishment in plasma, a two-stream instability and the Landau damping. Also, the effect of the calculating parameters on the solution was investigated.

References

- [1] Burdakov A.V., Postupaev V.V. Special features of heat transport with beam plasma heating in experiments with GOL-3 installation.—Novosibirsk, 1992.—(Preprint / SB RAS INP; 9).
- [2] Burdakov A.V., Koidan V.S., Piffl V., Postupaev V.V., Raus J., Sunka P. Soft X-ray diagnostics in REB-plasma interaction experiments // Proc. 19th Intern. Conf. on Phenomena in Ionized Gases.—Belgrade, 1989.—Vol. 2.—P. 318.
- [3] Breyzman B.N. The joint REB-plasma interaction // Voprosy teorii plazmy.—Moscow: Energoatomizdat, 1987.—Vyp. 15.—P. 55.
- [4] Breyzman B.N., Yungvirt K. Dynamics of the supersonic Langmuir turbulence // Voprosy teorii plazmy.—Moscow: Energoatomizdat, 1990.—Vyp. 18.—P. 3.
- [5] Birdsall C.K., Langdon A.B. Plasma Physics via Computer Simulation.—Bristol: Hilger, 1991.
- [6] Berezin Y.A., Vshivkov V.A. The Particles method in Low-Density Plasma.—Novosibirsk: Nauka, 1980.
- [7] Grigoriev Y.N., Vshivkov V.A., Fedoruk M.P. Numerical Modeling by Particle-in-Cells Method.—Novosibirsk: SB RAS, 2004.
- [8] Vshivkov V.A., Vshivkov K.V., Dudnikova G.I. Algorithms of solving the problem of laser-impulse interaction with plasma // J. Computational Technologies.—2001.—Vol. 6, No. 2.—P. 47–63.

- [9] Langdon A.B., Lasinski B.F. Electromagnetic and relativistic plasma simulation models // Meth. Comput. Phys. — 1976. — Vol. 16. — P. 327–366.
- [10] Landau L.D., Lifshits E.N. Field Theory: Theoretical Physics Series. Vol. 2. — Moscow: Nauka. Chief Editorial Board of Physico-Mathematical Literature, 1973.
- [11] Yavorski B.M. Detlaf A.A. A Handbook of Physics for Engineers and Students. — Moscow: State Publishing House of Physico-Mathematical Literature, 1963.